Hindawi
International Journal of Aerospace Engineering
Volume 2017, Article ID 8536732, 9 pages
https://doi.org/10.1155/2017/8536732

Research Article

Shorter Path Design and Control for an Underactuated Satellite

Jung-Hyung Lee,[1] Donghoon Kim,[2] Jichul Kim,[3] and Hwa-Suk Oh[1]

[1]*Department of Aerospace and Mechanical Engineering, Korea Aerospace University, Goyang, Republic of Korea*
[2]*Department of Aerospace Engineering, Mississippi State University, Mississippi State, MS, USA*
[3]*Aeronautical Engineering & Technology Division, Research Institute of Aerospace Engineering & Technology, Goyang, Republic of Korea*

Correspondence should be addressed to Donghoon Kim; donghoon38.kim@gmail.com

Received 27 April 2017; Revised 21 July 2017; Accepted 5 September 2017; Published 17 December 2017

Academic Editor: Christopher J. Damaren

In the event of a control failure on an axis of a spacecraft, a target attitude can be achieved by several sequential rotations around the remaining control axes. For a spacecraft actuating with wheels, the form of each submaneuver should be a pure single axis rotation since the failed axis should not be perturbed. The rotation path length in sequential submaneuvers, however, increases extremely but is short under normal conditions. In this work, it is shown that the path length is reduced dramatically by finding a proper number of sequential submaneuvers, especially for the target attitude rotation around the failed axis. A numerical optimization is suggested to obtain the shortest path length and the relevant number of maneuvers. Optimal solutions using the sequential rotation approach are confirmed by numerical simulations.

1. Introduction

A spacecraft attitude is controlled by actuators, which produce either external or internal torque depending on their types. For three-dimensional (3D) maneuvers, the control should be provided for all three axes [1, 2]. Failures in some actuators sometimes result in the complete control failure in an axis. In this case, proper contingency control laws should be provided to avoid the loss of controllability or stability in the axis. Many studies in the literature have introduced strategies to handle this kind of an underactuated system [3–6]. Control loss in an axis direction leads to a detour to achieve a target attitude using the remaining controllable actuators [7].

In Euler's theorem, an attitude can be represented by a single rotation angle about a principal axis, called the *eigen-axis*, or three sequential rotation angles, called the Euler angles. A rest-to-rest maneuver to a target attitude can then be performed by either an eigen-axis maneuver or three sequential principal submaneuvers following Euler angle sequences. In case of actuator failures, however, achieving a target attitude through an eigen-axis maneuver directly is impossible when the eigen-axis includes a component of the failed axis direction. In that case, several maneuvers should be performed by some submaneuvers around the remaining control axes only, either sequentially or concurrently. Due to the uncontrollability of the angular velocity space in the failed wheel system, the failed axis should not be perturbed during maneuvers [3, 4]. In this paper, the study is confined to a spacecraft system actuating with wheels, and thus, the submaneuvers considered here should be principal axis rotations.

In the rotation maneuvers, the magnitude of rotation angles is defined as a path length, and the shortest path can be obtained by the eigen-axis rotation [8–14]. The path length of sequential submaneuvers in failure modes increases significantly, longer than the one under normal conditions. To achieve an arbitrary target attitude around the failed axis, at least three sequential rotations must be performed around the remaining control axes. When three submaneuvers are used, they are uniquely determined, as is their total path length. If more than three submaneuvers are allowed, however, there exist a choice of paths and a possibility of the path length reduction. Both minimizing the path

length and finding the number of maneuvers are the key findings in this paper.

In Section 2, conditions for submaneuvers are considered to avert perturbations on the failed axis. In Section 3, a shorter path length is found through a numerical optimization approach. Finally, in Section 4, optimal solutions are confirmed to obtain the minimum path length and the relevant number of maneuvers by numerical simulations.

2. A Target Attitude Achievement

2.1. Principal Rotations. To describe motions of a spacecraft with four reaction wheels, a pyramid configuration is shown in Figure 1. The spacecraft's motion is governed by the following equations [2]:

$$\dot{\mathbf{q}} = \frac{1}{2}E(\mathbf{q})\dot{\boldsymbol{\omega}}, \quad E(\mathbf{q}) = \begin{bmatrix} q_4 & -q_3 & q_2 \\ q_3 & q_4 & -q_1 \\ -q_2 & q_1 & q_4 \\ -q_1 & -q_2 & -q_3 \end{bmatrix}, \tag{1}$$

$$I\dot{\boldsymbol{\omega}} = -\boldsymbol{\omega}^{\times}(I\boldsymbol{\omega} + A\mathbf{h}) + \mathbf{u}_c,$$
$$A = \begin{bmatrix} s\beta & s\beta & s\beta & s\beta \\ 0 & -c\beta & 0 & c\beta \\ c\beta & 0 & -c\beta & 0 \end{bmatrix}, \tag{2}$$

$$A\dot{\mathbf{h}} = -\mathbf{u}_c, \tag{3}$$

where $\mathbf{q} \in R^4$ is the attitude quaternion, $\boldsymbol{\omega} \in R^3$ is the spacecraft's angular velocity, the superscript $\times$ is the cross product symbol, and $\mathbf{u}_c \in R^3$ is the control torque generated by changing the wheel momentum $\mathbf{h} \in R^4$. The moment of inertia $I \in R^{3\times3}$ is assumed to have diagonal terms only; $A \in R^{3\times4}$ is the wheel configuration matrix composed of the wheel axis vectors $\hat{\mathbf{a}}_i \in R^3$ ($i = 1, 2, 3$, and 4); s and c denote the sine and cosine functions, respectively; β is the skew angle of the pyramid configuration; and then $A\mathbf{h} \in R^3$ represents the sum of wheel momentum. To achieve the target attitude $\mathbf{q}_t \in R^4$, a conventional quaternion feedback control law and a minimum norm steering law are presented as follows [8, 13]:

$$\mathbf{u}_C = \boldsymbol{\omega}^{\times}(I\boldsymbol{\omega} + A\mathbf{h}) - D\boldsymbol{\omega} + KE^T(\mathbf{q})\mathbf{q}_t, \tag{4}$$

$$\dot{\mathbf{h}} = -A^{+}\mathbf{u}_c, \tag{5}$$

where $D \in R^{3\times3}$ and $K \in R^{3\times3}$ are the gain matrices, respectively, and $A^+ \in R^{4\times3}$ is the pseudo inverse of A.

In general, the shortest path is obtained by a principal eigen-axis rotation. To perform a principal rotation around a specific axis in a rest-to-rest maneuver, the gyroscopic term $\boldsymbol{\omega}^{\times}(I\boldsymbol{\omega} + A\mathbf{h})$ in (2) should have no such component on the other axes so as not to induce movements on the axes. The magnitude of the rotation angle around an axis is defined as the path length of the rotation. The wheels accelerate or decelerate following the rotation angle and the angular velocity during the rotation maneuver.

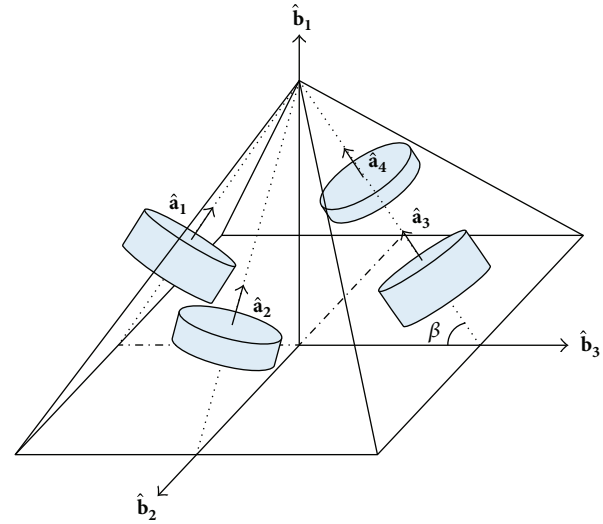

Figure 1: Spacecraft with four reaction wheels in a pyramid configuration.

2.2. Detour Paths in Failure Mode. On the pyramid-configured installation as shown in Figure 1, the axis $\hat{\mathbf{b}}_1$ is more robust in the aspect of control than the axes $\hat{\mathbf{b}}_2$ and $\hat{\mathbf{b}}_3$. In the event of failures in both wheels 1 and 3, for example, then, the control of the axis $\hat{\mathbf{b}}_3$ will be lost. Then, the required maneuver torque should be generated only by the remaining two wheels, 2 and 4, and the spacecraft turns into the underactuated system. Any rotation about the failed axis $\hat{\mathbf{b}}_3$ should be substituted by the submaneuvering rotations about the remaining two axes. Due to the uncontrollability of the angular velocity space in the failed wheel system, the failed axis should not be perturbed during maneuvers. The rotations should be performed sequentially around each single axis, not around both live axes simultaneously. The gyroscopic term $\boldsymbol{\omega}^{\times}A\mathbf{h}$ in (4) will not have the component on the failed axis if a principal rotation is performed around only one of the unfailed axes.

To achieve a target attitude (ψ, θ, ϕ) in the 3-2-1 set of Euler angles where the failed axis angle is $\psi \neq 0$, at least three sequential principal rotations (e.g., 1-2-1 or 2-1-2) must be performed. Using the direction cosine matrix of the target attitude, the 1-2-1 set of target Euler angles $(\phi', \vartheta, \phi'')$ and the 2-1-2 set of target Euler angles $(\vartheta', \varphi, \vartheta'')$ can be expressed as

$$\left(\phi', \vartheta, \phi''\right) = \left(-\mathrm{t}^{-1}\left(\frac{c\theta s\psi}{-s\theta}\right), \mathrm{c}^{-1}(c\theta c\psi), \mathrm{t}^{-1}\left(\frac{s\phi s\theta c\psi - c\phi s\psi}{c\phi s\theta c\psi + s\phi s\psi}\right)\right), \tag{6}$$

$$\left(\vartheta', \varphi, \vartheta''\right) = \left(\mathrm{t}^{-1}\left(\frac{s\phi s\theta c\psi - c\phi s\psi}{s\phi c\theta}\right), \mathrm{c}^{-1}(s\phi s\theta s\psi + c\phi c\psi), -\mathrm{t}^{-1}\left(\frac{c\theta s\psi}{c\phi s\theta s\psi - s\phi c\psi}\right)\right), \tag{7}$$

where t denotes the tangent function. Note that the derivation procedure of (6) and (7) is described in Appendix.

For the sequential rotations, the total path length is defined as the sum of the absolute value of principal rotation angles.

$$L_{1\text{-}2\text{-}1} \equiv \left|\phi'\right| + |\vartheta| + \left|\phi''\right|,$$
$$L_{2\text{-}1\text{-}2} \equiv \left|\vartheta'\right| + |\varphi| + \left|\vartheta''\right|. \tag{8}$$

For example, to achieve the attitude $(\psi, 0, 0)$ in a 3-2-1 Euler angle sense where the path length is $L_{3\text{-}2\text{-}1} = \psi$, the sequential rotation angles, the path lengths, and the path length differences compared to those of the principal angle rotation under the normal condition are presented as

$$\left(\phi', \vartheta, \phi''\right) = (90, \psi, -90) \text{ degrees},$$
$$L_{1\text{-}2\text{-}1} = \psi^\circ + 180^\circ, \tag{9}$$

$$\left(\vartheta', \varphi, \vartheta''\right) = (-90, \psi, 90) \text{ degrees},$$
$$L_{2\text{-}1\text{-}2} = \psi^\circ + 180^\circ, \tag{10}$$

$$\Delta L = L_{1\text{-}2\text{-}1} - L_{3\text{-}2\text{-}1} = L_{2\text{-}1\text{-}2} - L_{3\text{-}2\text{-}1} = 180^\circ. \tag{11}$$

At this point, a question arises whether any shorter path exists than the path from the three submaneuvers.

2.3. Existence of Shorter Paths. To simply demonstrate a shorter path existence, two cases are considered: (1) a rotation angle exists only on the failed control axis and (2) rotation angles exist around all the axes including the failed axis. For the first case, target (30, 0, 0) degrees in the 3-2-1 set of Euler angles are assumed, and the path length is found as 210 degrees from (9) and (10). To find the length of a shorter path, for example, consider target (30, 30, 0) degrees in the 3-2-1 set. The 1-2-1 set of target Euler angles is found using (6) as follows:

$$(30, 30, 0) \text{ degrees in the 3-2-1 set} \rightarrow (40.9, 41.4, -49.1) \text{ degrees in the 1-2-1 set.} \tag{12}$$

Then, the target attitude can be achieved by conducting an additional −30-degree rotation about the axis $\widehat{\mathbf{b}}_2$ as

$$(30, 0, 0) \text{ degrees the in 3-2-1 set} = (40.9, 41.4, -49.1, -30) \text{ degrees in the 1-2-1-2 set.} \tag{13}$$

Consequently, the path angle using the 1-2-1-2 set is found as 161.4 degrees, which is 48.6 degrees shorter than the one using the 1-2-1 set. That is, by applying more than three submaneuvers, the path length can be decreased. How about five submaneuvers then? Let us consider the second case when a target (30, 10, 10) in the 3-2-1 set of Euler angles is given. Using (6), (7), and (8), both 1-2-1 and 2-1-2 sets of Euler angles are obtained with the path lengths as follows:

$$(30, 10, 10) \text{ degrees in the 3-2-1 set} \rightarrow \begin{cases} (70.6, 31.5, -63.6) \text{ degrees in the 1-2-1 set}, & L_{1\text{-}2\text{-}1} = 165.4^\circ, \\ (-69.6, 29.8, 82.5) \text{ degrees in the 2-1-2 set}, & L_{2\text{-}1\text{-}2} = 182.1^\circ. \end{cases} \tag{14}$$

For this case, the target (30, 30, 0) degrees in the 3-2-1 set are also considered. Target attitude (30, 10, 0) degrees are obtained by conducting an additional −20-degree rotation about the $\widehat{\mathbf{b}}_2$ as follows:

$$(30, 10, 0) \text{ degrees in the 3-2-1 set} \rightarrow (40.9, 41.4, -49.1, -20) \text{ degrees in the 1-2-1-2 set.} \tag{15}$$

Then, the target attitude can be achieved by conducting an additional 10-degree rotation about the axis $\widehat{\mathbf{b}}_1$ as

$$(30, 10, 10) \text{ degrees in the 3-2-1 set} = (40.9, 41.4, -49.1, -20, 10) \text{ degrees in the 1-2-1-2-1 set.} \tag{16}$$

Consequently, the path angle using the 1-2-1-2-1 set is found as 161.4 degrees. This path angle is 4 degrees shorter than the one using the 1-2-1 set, and the path angle is 20.7 degrees shorter than the one using the 2-1-2 set.

Including the failed axis, the target attitude is approached by more than, or equal to, three submaneuvers. The solutions for the shortest path are not unique and can be obtained differently. The procedure to find a minimum path length, including the number of maneuvers, is explained in the following section.

3. Shorter Path Design

3.1. Quaternion Views. In Euler's theorem, any target, which can be approached by a single rotation (principal angle) about the eigen-axis, can also be approached by three sequential principal rotations (Euler angles). Suppose $\mathbf{q}_t = [q_{t,1}\ q_{t,2}\ q_{t,3}\ q_{t,4}]^T$ is approached by several sequential principal rotations from the initial attitude $\mathbf{q}_i = [0\ 0\ 0\ 1]^T$ at the inertial frame as

$$\mathbf{q}_t = Q_{p_n}^{(n)} Q_{p_{n-1}}^{(n-1)} \cdots Q_{p_k}^{(k)} \cdots Q_{p_2}^{(2)} Q_{p_1}^{(1)} \mathbf{q}_i, \tag{17}$$

where k is the rotation order, n is the maneuver numbers, and p_k is the unfailed axis number, and (17) must satisfy the quaternion constraint $\mathbf{q}_t^T \mathbf{q}_t = 1$. Then,

$$Q_{p_k}^{(k)} = \begin{bmatrix} q_4(\phi_k) & q_3(\phi_k) & -q_2(\phi_k) & q_1(\phi_k) \\ -q_3(\phi_k) & q_4(\phi_k) & q_1(\phi_k) & q_2(\phi_k) \\ q_2(\phi_k) & -q_1(\phi_k) & q_4(\phi_k) & q_3(\phi_k) \\ -q_1(\phi_k) & -q_2(\phi_k) & -q_3(\phi_k) & q_4(\phi_k) \end{bmatrix}, \quad (18)$$

and the elements are defined as

$$q_j(\phi_k) = \begin{cases} \mathrm{s}\dfrac{\phi_k}{2}, & j = p_k; \\ 0, & j \neq p_k; \\ \mathrm{c}\dfrac{\phi_k}{2}, & j = 4, \end{cases} \quad (19)$$

where ϕ_k is the kth principal angle of the unfailed axis.

On the failure in the axis $\hat{\mathbf{b}}_3$, $\mathbf{q}_t$ should be approached by rotations around the axis $\hat{\mathbf{b}}_1$ and/or $\hat{\mathbf{b}}_2$. For example, if the target attitude is approached by (1-2-1) rotations, then, the target attitude is

$$\mathbf{q}_t = Q_{p_3}^{(3)}(\phi_3) Q_{p_2}^{(2)}(\phi_2) Q_{p_1}^{(1)}(\phi_1) \mathbf{q}_i, \quad (20)$$

where

$$Q_{p_1}^{(1)}(\phi_1) = \begin{bmatrix} q_4(\phi_1) & 0 & 0 & q_1(\phi_1) \\ 0 & q_4(\phi_1) & q_1(\phi_1) & 0 \\ 0 & -q_1(\phi_1) & q_4(\phi_1) & 0 \\ -q_1(\phi_1) & 0 & 0 & q_4(\phi_1) \end{bmatrix},$$

$$Q_{p_2}^{(2)}(\phi_2) = \begin{bmatrix} q_4(\phi_2) & 0 & -q_2(\phi_2) & 0 \\ 0 & q_4(\phi_2) & 0 & q_2(\phi_2) \\ q_2(\phi_2) & 0 & q_4(\phi_2) & 0 \\ 0 & -q_2(\phi_2) & 0 & q_4(\phi_2) \end{bmatrix},$$

$$Q_{p_3}^{(3)}(\phi_3) = \begin{bmatrix} q_4(\phi_3) & 0 & 0 & q_1(\phi_3) \\ 0 & q_4(\phi_3) & q_1(\phi_3) & 0 \\ 0 & -q_1(\phi_3) & q_4(\phi_3) & 0 \\ -q_1(\phi_3) & 0 & 0 & q_4(\phi_3) \end{bmatrix}. \quad (21)$$

3.2. Search for the Shortest Path. To find the optimal solution of L^*, n^*, and ϕ_k^*, which minimizes the performance index in (8), the problem is defined as

$$\min L(n, \phi_1, \ldots, \phi_n) \equiv \min \sum_{k=1}^{n} |\phi_k|, \quad (22)$$

$$\text{subject to } L(n_{\text{normal}}) < L^*(n) \leq L \quad (n = 3), \quad (23)$$

$$\mathrm{c}\left(\mathbf{q}_i, \mathbf{q}_t, Q_{p_1}^{(1)}, \ldots, Q_{p_n}^{(n)}\right) = 0, \quad (24)$$

Table 1: Numerical simulation parameters.

Parameters	Symbol	Value	Units
Moment of inertia for the spacecraft	I	diag [200 120 130]	kg·m^2
Skew angle	β	53.13	deg
Control gains	K	diag [5 5 5]	—
	D	diag [45 35 36]	—
Maximum number of maneuver	$n_{\max}$	8	—
Failed axis	$\hat{\mathbf{b}}_3$	—	—

where $L(n_{\text{normal}})$ is the principal angle between the initial and the target attitudes approached by an eigen-axis rotation under the normal condition.

The path differs depending on the number of submaneuvers. Among the many paths to the target, there exist a shorter path length and the relevant number of maneuvers as shown in the previous section. Since there may be many local minimum paths, the initial guessing is substantial to secure the global minimum path solution. In this work, the length of the eigen-axis rotation under the normal condition divided by the maneuver number is used as an initial guess. After that, the found solution is used as a new initial guess to find the global minimum solution by redefining the maximum length of the inequality condition, which is the upper boundary in (23), to the obtained length. This procedure is continuously conducted until no solution exists, and the last solution is confirmed as the global minimum solution in the manner of using the sequential rotation approach. A more efficient way to find the global minimum solution needs to be studied. One can use any numerical tools to solve the optimization problems in (22) [12].

4. Optimization for the Shortest Path

4.1. Optimal Solutions with n Submaneuver Constraint ($n_{\text{normal}} \leq n \leq n_{\max}$). Equation (24) describes the constraint in (17), and this equation can be written for n submaneuver cases as follows:

$$q_{t,j} - r_j(\phi_n) \cdots f_j(\phi_3) g_j(\phi_2) h_j(\phi_1) = 0, \quad (j = 1, 2, 3, \text{and } 4), \quad (25)$$

where r_j, f_j, g_j, and h_j are the functions of n maneuvers which includes n unknowns and the quaternion constraint. Again, when $n = 3$, the rotation angles are uniquely determined. When $n > 3$, however, many possible solutions exist. To find the minimum of the constrained nonlinear multivariable function, Matlab function *fmincon*, which is the one of the nonlinear programming solvers, is utilized.

4.2. Numerical Results. The numerical simulation is performed for both cases mentioned in Section 2.3 using the parameters listed in Table 1. For the sequential maneuver, the following sets of maneuvers are considered: 1-2-1-… sets and 2-1-2-… sets. For both cases, the goal is

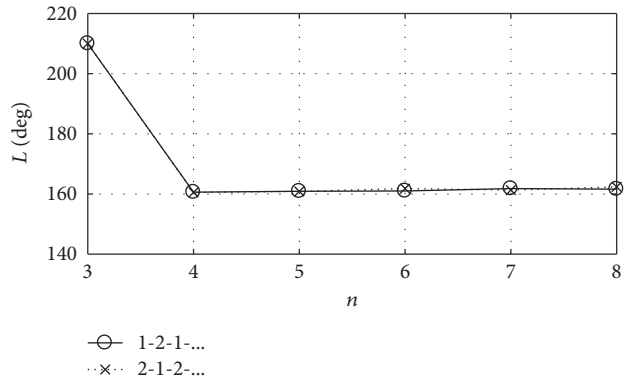

Figure 2: Path lengths according to the number of maneuvers for case 1.

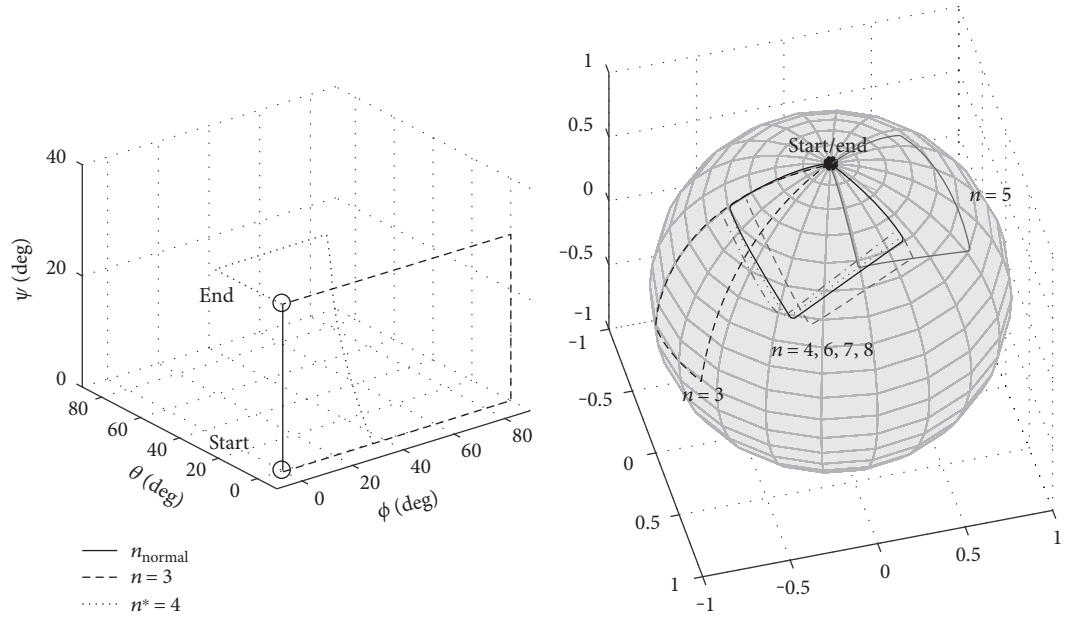

(a) 3D trajectories of the Euler angles

(b) Tendency of the path on a unit sphere

Figure 3: 3D trajectories and tendency descriptions for case 1.

to find the minimum path L^* according to the optimal number of maneuvers $n^*(n_{\text{normal}} \le n^* \le n_{\max})$ and the set of rotation angles ϕ_k^*.

In case 1, $L^* = 160.6^\circ$ is obtained when $n^* = 4$, regardless of using the 1-2-1-… set and 2-1-2-… set of maneuvers as shown in Figure 2. Figure 3(a) shows the 3D trajectories in terms of the 3-2-1 Euler angle sense according to the number of maneuvers. From the path length perspective, the trajectory of the $n^* = 4$ maneuvers is more efficient than the one of the $n = 3$ maneuvers. Figure 3(b) represents the path trends according to the number of maneuvers based on the 1-2-1-… set. *Note that a unit sphere is considered to simply provide the path tendency*. The similar path tendency is observed at $n = 4, 6, 7,$ and 8. As shown in Figure 3(b) and Table 2, some parts of the submaneuvers at $n = 6, 7,$ and 8 are close to zero. This means that the found solutions are local optimal solutions around the optimal solution, which is found at $n^* = 4$ and described with a bold line.

In case 2, $L^* = 143.5^\circ$ is obtained when $n^* = 4$ using the 2-1-2-… set maneuver as shown in Figure 4. Figure 5(a) shows the 3D trajectories in terms of the 3-2-1 Euler angle sense according to the number of maneuvers, and the $n^* = 4$ maneuvers are more efficient than the $n = 3$ maneuvers from the path length perspective. Figure 5(b) represents the path trends according to the number of maneuvers based on the 2-1-2-… set. As shown in Figure 5(b) and Table 3, the similar path tendency is observed when $n = 4$~8, respectively. These are the local optimal solutions, and the solution providing the minimum path when $n^* = 4$ is described with a bold line.

Consequently, the optimal solutions found for both cases 1 and 2 are listed in Tables 2 and 3, respectively. When the rotation angle exists only on the failed control axis, the shortest path is obtained for both 1-2-1-… set and 2-1-2-… set of maneuvers. When the rotation angles exist around the all axes, an optimal maneuver set is obtained.

Table 2: Initial and obtained sets of a target attitude for case 1.

State		Euler angle	n	$[\phi_1, \ldots, \phi_n]$ (deg)	L (deg)
Initial attitude	—	3-2-1 set	—	[0.0 0.0 0.0]	—
Target attitude	Normal	3-2-1 set	1	[30.0 0.0 0.0]	30.0
		1-2-1-… set	3	[90.0 30.0 −90.0]	210.0
			4	[35.3 45.0 −45.0 −35.3]	160.6
			5	[0.6 38.1 −43.3 −46.8 32.1]	160.9
			6	[35.6 12.0 0.8 32.3 −46.0 −34.3]	161.0
			7	[38.7 43.2 −20.2 −0.7 −27.2 −31.7 −0.1]	161.6
			8	[−29.4 −49.7 39.7 2.1 0.7 9.2 0.5 30.3]	161.6
	Failure 3-axis	2-1-2-… set	3	[−90.0 30.0 90.0]	210.0
			4	[−35.3 45.0 45.0 −35.3]	160.6
			5	[35.0 −44.6 −45.4 35.1 0.8]	160.9
			6	[−39.5 29.6 1.5 12.9 46.6 −31.7]	161.8
			7	[−0.0 −35.2 −44.1 46.0 32.0 −1.2 2.7]	161.2
			8	[−33.8 46.5 40.6 −1.5 −0.5 −3.1 3.8 −32.5]	162.3

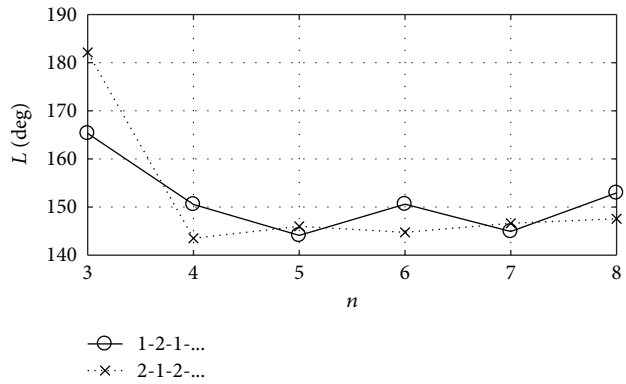

Figure 4: Path lengths according to the number of maneuvers for case 2.

Figure 6 presents the optimal values of n^* given $\psi = 30^\circ$, $0^\circ < \theta < 90^\circ$, $0^\circ < \phi < 90^\circ$ conditions and angle intervals $\Delta\theta = \Delta\phi = 10^\circ$. Note that the results are symmetric at negative angle ranges: $-90^\circ < \theta < 0^\circ$ and $-90^\circ < \phi < 0^\circ$. Consequently, the minimum path length is found by performing three or four sequential maneuvers. That is, $n^* = 3$ or 4. Figure 7(a) illustrates the path gaps between the solution under the normal condition and the three sequential maneuvers given the failed axis $\hat{\mathbf{b}}_3$. When θ and ϕ approach to zero, the magnitude of the path gap increases. It means that the total path length of $n = 3$ maneuvers becomes long because additional rotations around the live axes were required. When θ and ϕ approach to about 50°, the magnitude of the path gap decreases. It means that $n = 3$ maneuvers that include rotation angles around the live axes are somewhat similar to the principal angle rotation under the normal condition. When θ and ϕ approach to about 90°, the magnitude of the path gap tends to slightly increase. Figure 7(b) presents the available minimum path lengths between $n = 3$ maneuvers and maneuvers under the normal condition. The minimum path length found by the 1-2-1-… set maneuver is marked with the circle sign (o), one found by the 2-1-2-… set maneuver is marked with the plus sign (+), and one found by the both sets is marked with the asterisk sign (∗). Consequently, the graph shows that there may exist potential rooms to have better solutions using different methods.

5. Conclusion

In the control failure of an axis, an arbitrary target attitude can be approached through several paths. The target is achieved by conducting some submaneuvers with the remaining control in the live axes with the cost of the path length increase. The existence of a path of the minimum length and the number of maneuvers is found, and it is confirmed by numerically performing some example maneuvers. A numerical approach for finding the minimum path to a specific target attitude is shown, and the

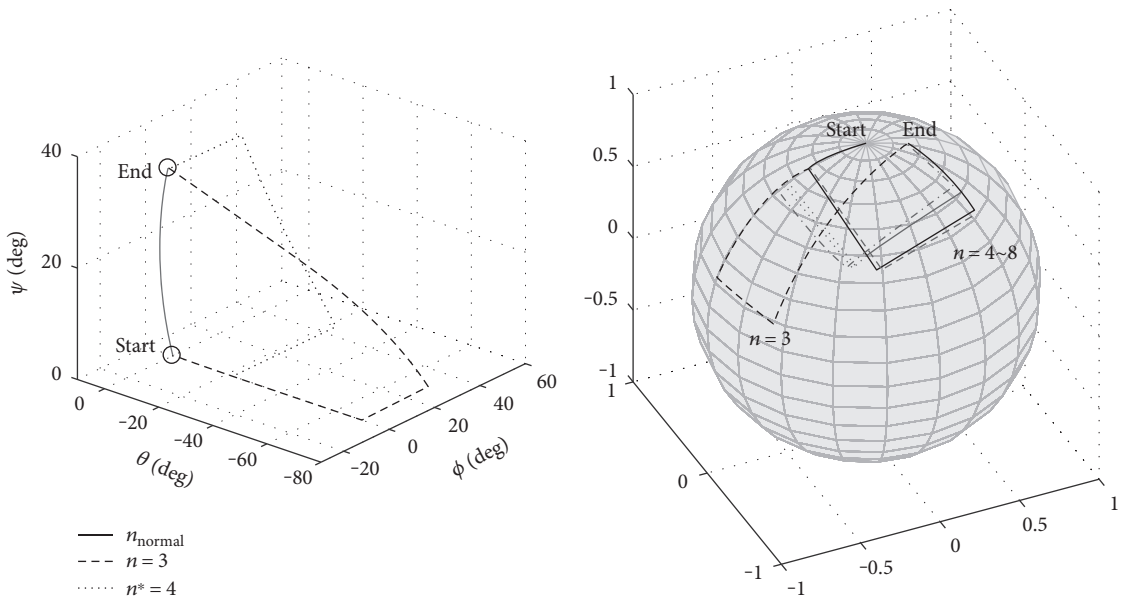

(a) 3D trajectories of the Euler angles

(b) Tendency of the path on a unit sphere

Figure 5: 3D trajectories and tendency descriptions for case 2.

Table 3: Initial and obtained sets of a target attitude for case 2.

State		Euler angle	n	$[\phi_1, \ldots, \phi_n]$ (deg)	L (deg)
Initial attitude	—	3-2-1 set	—	[0.0 0.0 0.0]	—
Target attitude	Normal	3-2-1 set	1	[30.0 10.0 10.0]	32.3
			3	[70.57 31.47 −63.26]	165.3
		1-2-1-… set	4	[46.07 42.63 −43.51 −18.33]	150.5
			5	[−0.34 −27.14 42.37 47.07 −27.19]	144.1
			6	[44.11 0.00 0.02 44.08 −42.09 −20.30]	150.6
			7	[0.00 −9.66 1.95 −15.79 41.76 46.29 −29.47]	144.9
			8	[0.00 −0.92 52.20 39.55 −43.76 −8.03 −3.98 −4.49]	152.9
	Failure 3-axis	2-1-2-… set	3	[−69.9 29.8 82.5]	182.2
			4	[−22.3 45.5 43.7 −32.0]	143.5
			5	[−30.5 40.8 48.7 −24.8 1.2]	146.0
			6	[−21.1 46.6 −0.3 −0.2 43.1 −33.3]	144.6
			7	[−33.4 39.0 15.8 −0.1 35.6 −22.2 0.6]	146.7
			8	[−30.0 19.8 −1.5 7.4 2.4 13.4 48.4 −24.9]	147.8

results are demonstrated and explained. It is found that the reduction of the path length is enormous when adapting four submaneuver strategies, especially for the case where the target attitude exists about the failed axis. In addition, the minimum path is always observed when three and/or four sequential maneuvers are conducted. The suggested approach will be useful to perform 3D missions considering energy savings.

Appendix

A special set of Euler angles to avoid an input to the failed axis $\hat{\mathbf{b}}_3$ is derived. Suppose that the direction cosine matrix of the target attitude is given as $C \in R^{3\times3}$, (6) and (7) can be obtained as

$$\begin{aligned}\left(\phi', \vartheta, \phi''\right) &= \left(-\mathrm{t}^{-1}\left(\frac{C(1,2)}{C(1,3)}\right), \mathrm{c}^{-1}(C(1,1)),\right.\\ &\qquad \left.\mathrm{t}^{-1}\left(\frac{C(2,1)}{C(3,1)}\right)\right),\\ \left(\vartheta', \varphi, \vartheta''\right) &= \left(\mathrm{t}^{-1}\left(\frac{C(2,1)}{C(2,3)}\right), \mathrm{c}^{-1}(C(2,2)),\right.\\ &\qquad \left.-\mathrm{t}^{-1}\left(\frac{C(1,2)}{C(3,2)}\right)\right),\end{aligned} \tag{A.1}$$

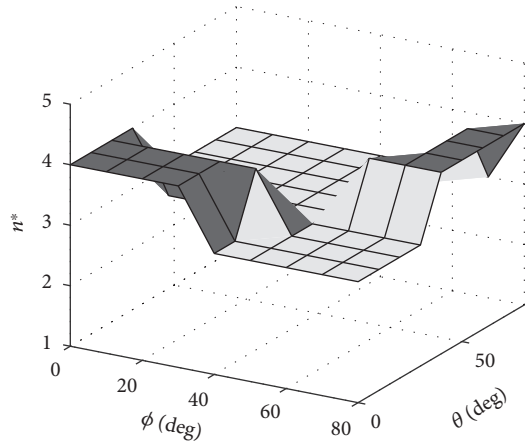

Figure 6: The minimum number of maneuvers given arbitrary target attitudes ($\psi = 30^\circ$).

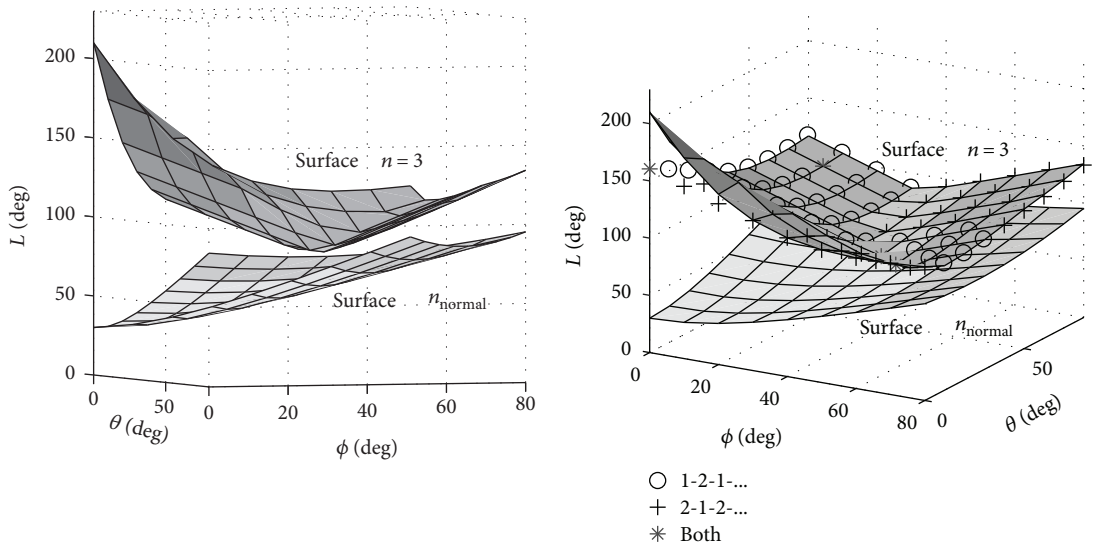

(a) Path gap description

(b) Available minimum path length surface description

Figure 7: Path length results for arbitrary target attitudes ($\psi = 30^\circ$).

where

$$C = \begin{bmatrix} c\theta c\psi & c\theta s\psi & -s\theta \\ s\phi s\theta c\psi - c\phi s\psi & s\phi s\theta s\psi + c\phi c\psi & s\phi c\theta \\ c\phi s\theta c\psi + s\phi s\psi & c\phi s\theta s\psi - s\phi c\psi & c\phi c\theta \end{bmatrix}. \quad (A.2)$$

When the failed control axis angle is ψ and $\theta = \phi$, (A.1) and (A.2) can be expressed as

$$\left(\phi', \vartheta, \phi''\right) = \left(-t^{-1}\left(\frac{c\phi s\psi}{-s\phi}\right), c^{-1}(c\phi c\psi), t^{-1}\left(\frac{s^2\phi c\psi - c\phi s\psi}{s\phi(c\phi c\psi + s\psi)}\right)\right),$$
$$\left(\vartheta', \varphi, \vartheta''\right) = \left(t^{-1}\left(\frac{s^2\phi c\psi - c\phi s\psi}{s\phi c\phi}\right), c^{-1}\left(s^2\phi s\psi + c\phi c\psi\right), - t^{-1}\left(\frac{c\phi s\psi}{s\phi(c\phi s\psi - c\psi)}\right)\right). \quad (A.3)$$

When $\psi = 30^\circ$, one can obtain the following as shown in (9) and (10):

$$\begin{aligned}\left(\phi', \vartheta, \phi''\right) &= \left(-t^{-1}(-\infty), c^{-1}(c\psi), t^{-1}(-\infty)\right) \\ &= (90, \psi, -90) \text{ degrees}, \\ \left(\vartheta', \varphi, \vartheta''\right) &= \left(t^{-1}(-\infty), c^{-1}(c\psi), -t^{-1}(-\infty)\right) \\ &= (-90, \psi, 90) \text{ degrees}.\end{aligned} \quad (A.4)$$

Conflicts of Interest

The authors declare that they have no conflicts of interest.

Acknowledgments

This work was supported by the Global Surveillance Research Center (GSRC) program funded by the Defense Acquisition

Program Administration (DAPA) and Agency for Defense Development (ADD).

References

[1] M. Sidi, *Spacecraft Dynamics and Control*, Cambridge University Press, UK, 1997.

[2] P. C. Hughes, *Spacecraft Attitude Dynamics*, Joh Wiley & Sons, Hoboken, New Jersey, USA, 1986.

[3] P. E. Crouch, "Spacecraft attitude control and stabilization: applications of geometric control theory to rigid body models," *IEEE Transactions on Automatic Control*, vol. 29, no. 4, pp. 321–331, 1984.

[4] P. Tsiotras and J. Luo, "Reduced effort control laws for underactuated rigid spacecraft," *Journal of Guidance, Control, and Dynamics*, vol. 20, no. 6, 1997.

[5] D. Kim, J. D. Turner, and H. Leeghim, "Reorientation of asymmetric rigid body using two controls," *Mathematical Problems in Engineering*, vol. 2013, Article ID 708935, 8 pages, 2013.

[6] D. Kim and J. D. Turner, "Near-minimum-time control of asymmetric rigid spacecraft using two controls," *Automatica*, vol. 50, 2014.

[7] D. Kim and H. Leeghim, "A new approach for handling underactuated system control," *Transactions of the Japan Society for Aeronautical and Space Sciences*, vol. 58, no. 2, pp. 110-111, 2015.

[8] B. Wie, H. Weiss, and A. Arapostathis, "Quarternion feedback regulator for spacecraft eigenaxis rotations," *Journal of Guidance, Control, and Dynamics*, vol. 12, no. 3, pp. 375–380, 1989.

[9] W. H. Steyn, "Near-minimum-time eigenaxis rotation maneuvers using reaction wheels," *Journal of Guidance, Control, and Dynamics*, vol. 18, no. 5, pp. 1184–1189, 1995.

[10] H.-S. Oh, Y.-D. Yoon, Y.-K. Chang, J.-H. Hwang, and S. S. Lim, "Near-eigenaxis rotation control law design for moving-to-rest maneuver," *Journal of Guidance, Control, and Dynamics*, vol. 24, no. 6, 2001.

[11] J. Lawton and R. Beard, "Attitude regulation about a fixed rotation axis," *Journal of Guidance, Control, and Dynamics*, vol. 26, no. 2, 2003.

[12] J. L. Junkins and J. D. Turner, *Optimal Spacecraft Rotational Maneuvers*, Elsevier Scientific Publishing Company, Amsterdam, The Netherlands, 1985.

[13] H. S. Oh and S. Vadali, "Feedback control and steering laws for spacecraft using single gimbal control moment gyros," *The Journal of the Astronautical Sciences*, vol. 39, pp. 183–203, 1991.

[14] H.-S. Oh, "Shorter rotation path design in underactuated wheel spacecraft," in *66th International Astronautical Congress*, Jerusalem, Israel, October 2015.